Supporting Information

for

Pd-mediated Synthesis of Ag_{33} Chiral Nanocluster with Core-shell Structure in T Point Group

Fan Tian, Rong Chen*

School of Chemistry and Environmental Engineering, Wuhan Institute of Technology, Xiongchu Avenue, Wuhan, 430073, PR China

** Corresponding author: Prof. R. Chen, E-mail: rchenhku@hotmail.com*

Tel.: (+86)13659815698; Fax: (+86)2787195680.

Chemicals

Silver nitrate ($AgNO_3$, AR), sodium borohydride (98%), methanol (MeOH, AR) and dichloromethane (CH_2Cl_2, AR) were purchased from Sinopharm (Shanghai, China). 2-phenylethanethiol ($PhCH_2CH_2SH$, 98%) was purchased from EnergyChemical(Shanghai, China). Triphenylphosphine (PPh_3, 99%), tetrakis(triphenylphosphine) palladium ($Pd(PPh_3)_4$, 99%) and bis(triphenylphosphine)palladium(II) dichloride ($(PPh)_2PdCl_2$, 98%) were purchased from Meryer (Shanghai, China). The water used in all experiments was ultrapure. All the reagents were used directly without further purification.

Methods

Synthesis of $Ag_{33}(SCH_2CH_2Ph)_{24}(PPh_3)_4$ nanoclusters: *120 mg $AgNO_3$ and 50 mg of $(PPh_3)_4PdCl_2$ were dispersed in 10 mL of methanol, followed by addition of 40 mL of dichloromethane, forming a grey black solution. The solution was stirred for 10 min following by 150 μL of $PhCH_2CH_2SH$ added in. After stirred for more than 1 hour to assure that all the metal atoms were fully coordinate with thiol, 500 mg of PPh_3 was added. The solution was stirring for another half an hour, and then 1 mL of an aqueous solution of $NaBH_4$ (60 mg/mL) was added in under vigorous stirring. The solution then quickly turned to reddish black, indicating the formation of nanoparticles. A purplish red solution was obtained after maintained the reaction under room temperature (20±3°C) for 24 hours. Purified Ag_{33} nanoparticles were separated out from the purplish-red solution by rotary evaporation and centrifugation. Dark single crystals suitable for X-ray diffraction study were grown by a double-layer of hexane/CH_2Cl_2 solution with suitable PPh_3 concentration of the purified products at 4 °C for two weeks.*

Characterization. *The UV-vis spectrum and photoluminescence spectrum were recorded by HITACHI UH4510 Spectrophotometer and FL 4600 fluorescence spectrophotometer with dichloromethane as solvent and 10 mg/mL PPh_3 stabilizing the nanoclusters, respectively. NMR spectrum were recorded at room temperature on a Bruker AV-500 spectrometer with chloroform-d_3 as solvent and TMS (0.0 ppm) as an internal reference, also in the presence of 10 mg/mL PPh_3 in the solution. X-ray diffraction data was recorded on an XtaLAB AFC12 (RINC): Kappa single diffractometer (Rigaku, Japan) with Cu Kα radiation (λ = 1.54184 Å). The crystal was kept at 100.00(10) K during data collection. Atomic absorption detector (AAS) was measured on an Elementab SOLAAR M6 (Thermo Scientific, USA) analytical instrument. Inductivity Coupled Plasma-Mass Spectrometry (ICP-MS) was measured on an Agilent 7700X (USA) instrument. X-ray photoelectron spectroscopy (XPS) was measured on an ESCALAB XI+ (Thermo Scientific, USA) photoelectron spectrometer*

using Al Kα radiation as the excitation source under vacuum at 2 × 10^{-6} Pa and all spectra were calibrated to the C 1s peak at 284.6 eV of the surface adventitious carbon. Circular dichroism (CD) spectrum was measured on a Chirascan Plus ECD spectrometer (Applied Photophysics, UK) with dichloromethane as solvent and 10 mg/mL PPh_3 stabilizing the nanoclusters.

Computational details: *DFT optimization was performed using the b3lyp hybrid density functional. We employed basis sets of 6–31 G** for H, C, P and S atoms by referring to the previous resport[1]. The LANL2DZ basis set was used for silver and palladium atoms. TD-DFT calculations of optical absorption spectra were performed and compared with experimental optical spectra. All calculations were carried out with Gaussian16 package[2]. Data extractions of the calculated results were processed with Multiwfn3.6 package[3].*

X-ray single-crystal analysis

A suitable crystal of Ag_{33} nanoparticles grown by a double-layer of hexane/CH_2Cl_2 solution with suitable PPh_3 concentration of the purified prouducts was selected and the diffraction data of the single crystals were collected on an on a XtaLAB AFC12 (RINC): Kappa single diffractometer(Rigaku, Japan) with Cu Kα radiation (λ = 1.54184 Å). The crystal was kept at 100.00(10) K during data collection. The data were processed and reduction using CrysAlisPro[4]. Using Olex2 [5], the structure was solved with the ShelXS [6] structure solution program using Direct Methods and refined with the ShelXL [7] refinement package using Least Squares minimization. Detailed crystal data and structure refinements for both compounds are provided in Supplementary Table S1.

NMR analysis

NMR spectrum of Ag_{33} nanocluster were recorded at room temperature on a Bruker AV-500 spectrometer with chloroform-d_3 as solvent and TMS (0.0 ppm) as an internal reference in the presence of 10 mg/mL PPh_3 in the solution. In the ^1H NMR spectrum of the Ag_{33} nanocluster in the region of 4.5-2.0 ppm, which corresponding to the methylene protons' resonance signals, seven peaks with integrals of 3:6:3:3:3:3:3 are observed (Figure S10 and Table S5). By referring to the crystal structure of Ag_{33} nanocluster, there are 96 methylene protons (96H) in total, therefore, each integral of "3" indicates 12H. The 24H for the peak at 3.48 ppm can resolved as two group of inequivalence protons occasionally overlapped and each group of 12H, which is verified by the corresponding ^1H-^{13}C HSQC (Figure 3c) spectra where the peaks at 3.48 ppm is indeed cross with two kind of carbon. We categorized all the 28 ligands of Ag_{33} nanocluster as two type of thiol ligands (type ***1***

*and type **2**) and one type of triphenylphosphine ligand (*PPh_3), as depicted by the crystallographic analysis. Then the inequivalent methylene groups of cluster can be classified as methylene group in type **1** ligand (subscript with **1**), in type **2** ligand (subscript with **2**) and in *PPh_3 (subscript with **p**). We assigned the left-most peak at 4.24 ppm in ^1H dimension as the first proton connecting to **α**-C in type **1** ligands, which labeled as $\boldsymbol{\alpha_{H1}}$, then the second proton in **α**-C should be at 2.64 ppm according to the ^1H-^{13}C HSQC spectrum (Figure 3c), and labeled as $\boldsymbol{\alpha_{H1}'}$. The remaining peaks at 3.30 and 2.43 ppm in ^1H-^1H COSY spectrum connected by blue dashlines (Figure 3b) therefore could be attributed to the protons in **β**-CH_2 of the identical ligand. We labeled them as $\boldsymbol{\beta_{H1}}$ and$\boldsymbol{\beta_{H1}'}$, respectively. Then all the peaks crossed by blue dashline (in Figure 3b) can self-consistent. Employing the same procedure for the peaks in green line (in Figure 3b) can index all protons connecting to **α**- and **β**- C atoms in type **2** ligands: 3.49 ppm, $\boldsymbol{\alpha_{H2}}$; 3.47 ppm, $\boldsymbol{\beta_{H2}}$; 3.16 ppm, $\boldsymbol{\alpha_{H2}'}$; 2.84 ppm, $\boldsymbol{\beta_{H2}'}$. (Figure 3a and Table S5).*

*The assignments of ^1H NMR peaks in the region of 7.5 ppm to 6.3 ppm seem slightly more trick because the overlapping between signals of phenyl protons of thiol ligands (type **1** and type **2**), coordinated triphenylphosphine ligands and dissociate (free) triphenylphosphine (denoted at PPh_3) in solution. We acquired the ^1H NMR and ^{13}C NMR of the dissociate PPh_3 as reference for the analysis (Figure S8 and S9). The resonance signal of protons in PPh_3 are a multiple peak centered at 7.35 ppm with full width of 0.1 ppm (Figure S8). Two doublet and one triplet peaks which centered at 128.6, 133.8 and 137.3 ppm for the resonance signals of C in PPh_3 (Figure S9). The acquisited ^1H NMR spectrum for Ag_{33} nanocluster presence a multiple peak associated with protons at 7.32 ppm, therefore can be concluded to mainly contribute from the dissociate PPh_3, while the other peaks in the region of 7.5 ppm to 6.3 ppm might be mainly contributed from Ag_{33} nanocluster (Figure S10). To further figure the contribution out, we compared the resonance intensities between ^1H NMR spectrum of two different concentration of Ag_{33} nanocluster. It is found that increasing the concentration of Ag_{33} nanoclusters from 30 mg/mL to 120 mg/mL would eventually induced an increasing intensity of all the peaks in the region of 2.0-7.5 ppm, demonstrating they are corresponding to Ag_{33} nanoclusters. Four times increasing integrals are observed for those peaks except the one centered at 7.32 ppm, indicating the peak at 7.32 ppm is partial contributed from Ag_{33} nanoclusters. According to the observation, we can safely conclude that the peak at 7.32 ppm is mainly contribution from the dissociate PPh_3. Furthermore, slightly overlapping of those signals with Ag_{33} of the peak is also verified. Therefore, we assigned the ^1H NMR peaks in the region of 7.5 ppm to 6.3 ppm firstly let the peak at 7.32 out of our consideration. The following doublet peak at 7.24 ppm is overlapping with impurity proton in $CDCl_3$ solvent. The corrected integral of*

this peak should be 6. Therefore, in the region between 7.3 to 6.2 ppm of ^{1}H NMR spectrum, seven peaks belonging to the nanocluster ligands at 7.24 (doublet), 7.06 (triplet), 6.95 (multiplet), 6.75 (triplet), 6.60 (triplet) and 6.45 (doublet) ppm with integral of 6:3:12:6:6:6 are present. Recalling that there are 276H for the Ag_{33} nanocluster. 96H and 180H are ascribed to methylene group and phenyl group respectively. The total integral of the seven peaks are account for 156H, therefore the rest 24H can be deduced to an peak area integral of 6, which overlapping with the signals of protons in the dissociate PPh_3 centered at 7.32 ppm.

*The inequivalent phenyl groups of cluster can be classified as phenyl group in type **1** ligand (subscript with **1**), in type **2** ligand (subscript with **2**) and in *PPh_3 (subscript with **p**) according to the crystallographic analysis. Each type of phenyl group possessing protons in **ortho**-positon (**o**-H), **meta**-positon (**m**-H) and **para**-positon (**p**-H) can contribute to ^{1}H NMR signal with integral of 6:6:3, respectively. Therefore, the three type of phenyl groups would produce three sets of peaks with each set consisted of three peaks (**o**-H, 24H; **m**-H, 24H, 2; **p**-H, 12H) and nine peaks in total. Treating the observed multiplet peak around 6.95 ppm as three peaks with integral of 3 (6.97 ppm), 6 (6.94 ppm), 3 (6.89 ppm) would perfectly reproduce the analysis. Therefore, we further check the corresponding ^{1}H-^{13}C HSQC spectrum (Figure 3e) to figure out whether it is true. We observed three cross-signals associated with multiplet peak around 6.95 ppm in the ^{1}H dimension, indicating it indeed overlapped by three peaks. Further assignment of those peaks need the corresponding ^{13}C spectrum providing more resonance information. The full range ^{13}C NMR spectrum shows that the resonance signals of C in Ag_{33} and PPh_3 are present in the range of 120-150 ppm (Figure S12). We exclude the C signals contributed from the dissociate PPh_3 by referring ^{13}C NMR spectrum of PPh_3 (Figure S9)and comparing the ^{13}C NMR spectrum of different concentration of Ag_{33} nanoclusters (Figure S13), The two doublet peaks at 128.5, 136.8 ppm and two singlet peaks at 133.71,133.86 ppm are ascribed to the dissociate PPh_3.*

*By figuring out all C and H signals associated with the impurity phenyl group, we can assign the peaks between 7.5 to 6.3 ppm in the ^{1}H NMR spectrum of Ag_{33} nanoclusters. By concentrating the assignment on the peaks at 7.06, 6.97 and 6.89 ppm with each integral of 3, we firstly assigned the most right one at 6.89 ppm as **p**-H in PPh_3 ligands ($\boldsymbol{p_{Hp}}$, 12H) because its correlated C signal in ^{13}C NMR spectrum is far away from the other two (Figure 3e). Then referring to the ^{1}H-^{1}H COSY spectrum (Figure 3d), we further assigned **o**-H ($\boldsymbol{o}_{HP}$) and **m**-H ($\boldsymbol{m}_{HP}$) in PPh_3 ligands as 7.32 ppm (overlapped with the signals of dissociate PPh_3) and 6.60 ppm, respectively. The assignment of peaks at 7.06 and 6.97 ppm seems troublesome for the same structure of the two type of ligands and the intricate chemical environment surrounding them. However, the corresponding ^{1}H-^{1}H COSY spectrum (Figure*

*3d) show that the correlated **o**-H signals present at 6.45 and 7.24 ppm. We attribute the distinct difference of the chemical shift for the two **o**-H owing to the H-π conjugation effect between PPh_3 ligands and the type **2** thiol ligands. Compared to type 1 ligand, the **o**-H in type **2** ligands are located in an extra ring current environment provided by the phenyl group of PPh_3 ligands owing to the H-π interaction, which may partially cancel the direct influence of the ring current effect provided by the phenyl ring of thiol, therefore induced a decreased deshielding effect for the protons. Assigning the signal at 6.45 ppm as the **o**-H in type **2** ligands ($\mathbf{o}_{H2}$), we further resolved the rest peaks as: 7.24,$\mathbf{o}_{H1}$; 7.06,$\mathbf{p}_{H2}$; 6.97, $\mathbf{p}_{H1}$; 6.94, $\mathbf{m}_{H2}$ and 6.75, $\mathbf{m}_{H1}$.*

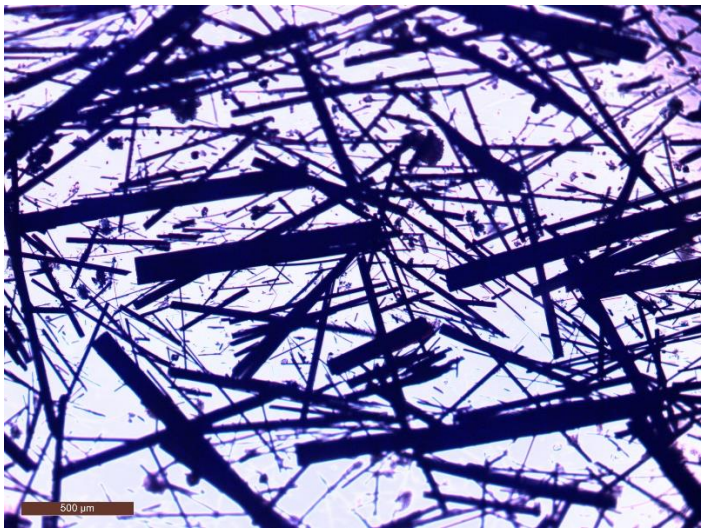

Figure S1 Photograph of black crystals growth in CH_2Cl_2/hexane.

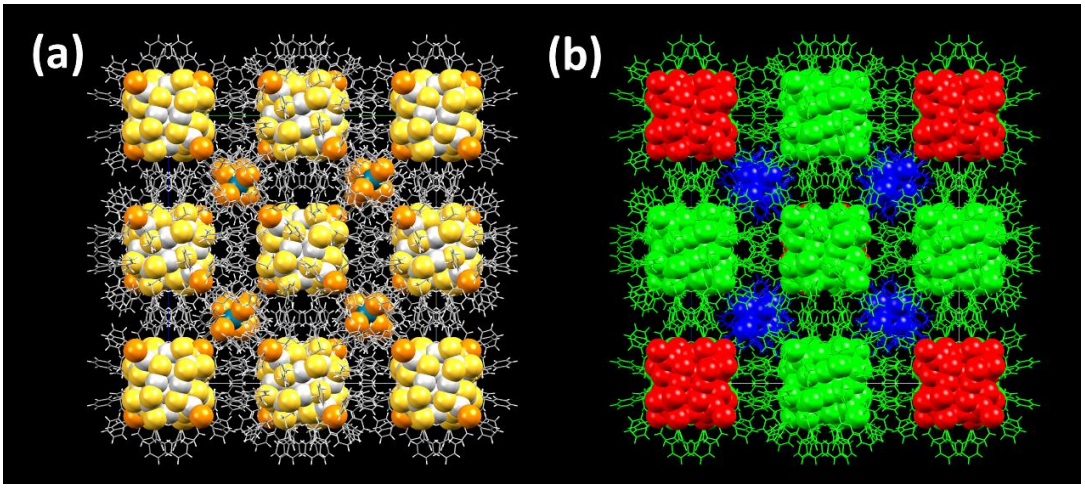

Figure S2 Crystal structure of Ag_{33} nanocluster with packing mode in a cell view down from crystallographic ***a*** axis: color by element (C: grey; S: yellow; Ag: sliver white; Pd: dark blue; P: orange; a) and by symmetry equivalence (b). The equivalent symmetries in red and green denote Ag_{33} enantiomers of anti-clockwise and clockwise screwing directions, respectively. Atoms in blue denotes $Pd(PPh_3)_4$/$Pd(PPh_3)_3Cl$ molecules. Recalling that the anti-clockwise enantiomers (in red) only partially occupy with site occupation of 0.25, C and H atoms in the molecule are missing owing to the low diffraction ability of those atoms.

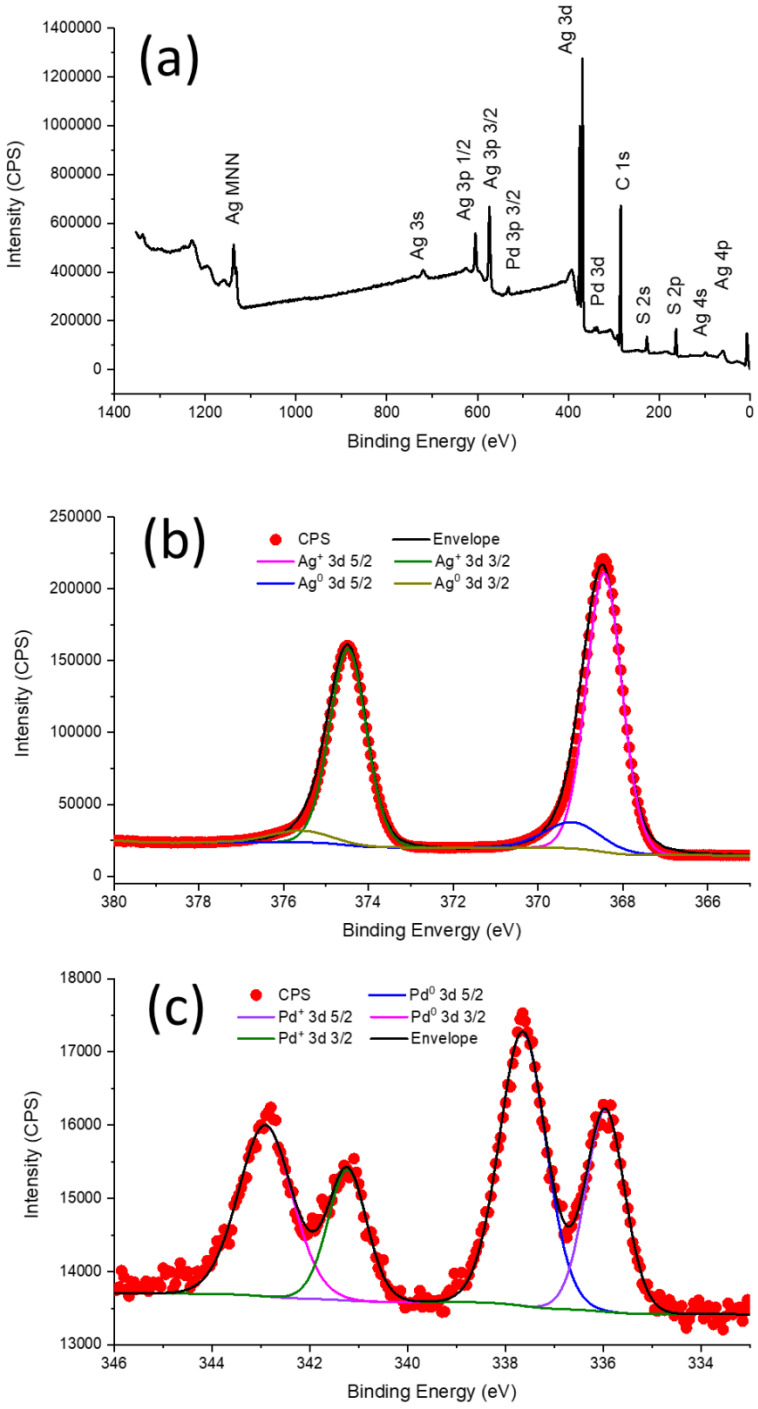

Figure S3 X-ray photoelectron spectra of the black crystals: survey spectrum (a), high-resolution spectra of Ag 3d (b) and Pd 3d (c).

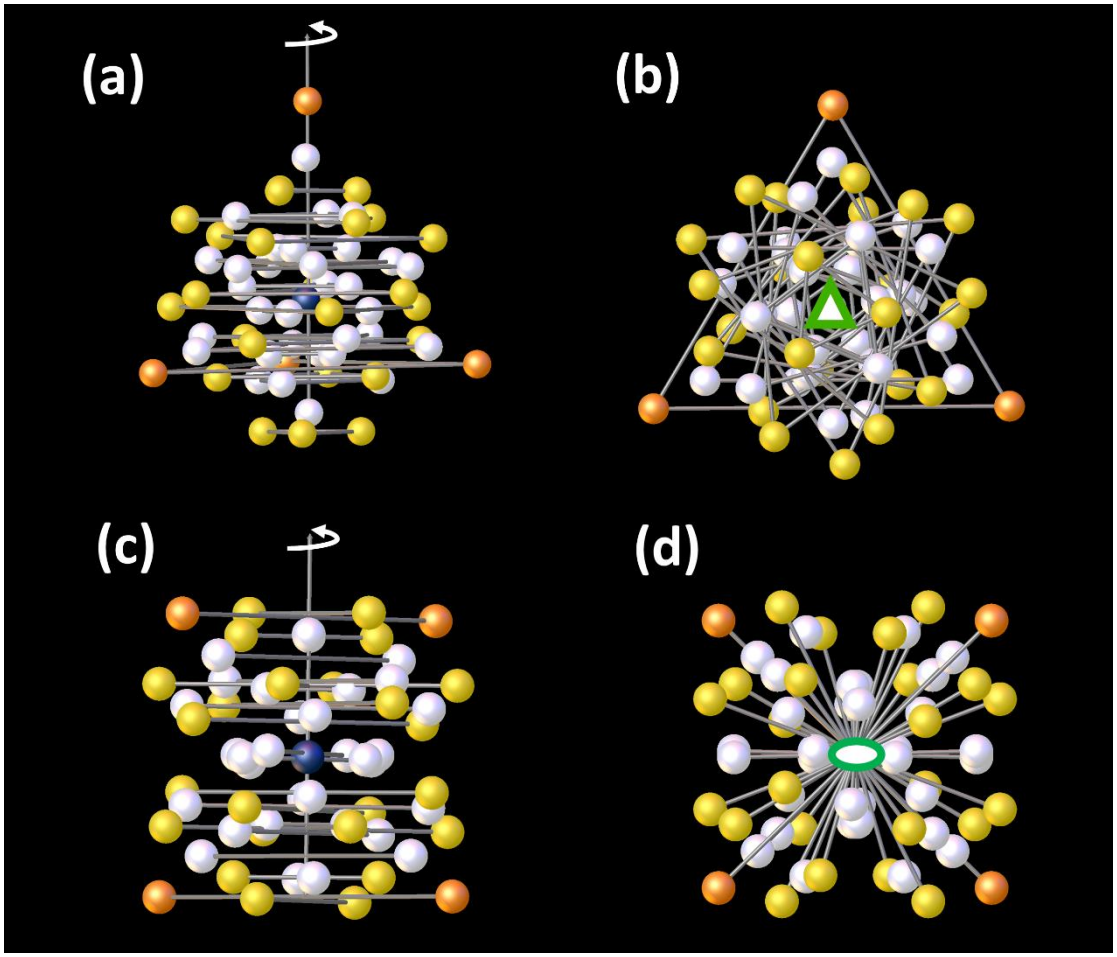

Figure S4 Rotational symmetries in the kernel of Ag_{33} nanoparticle: $\boldsymbol{C_3}$ symmetries views vertically against the axis (a) and along the axis (b); $\boldsymbol{C_2}$ symmetries views along the axis (c) and along the axis (d). Atoms in symmetrically equivalent sites are connect with line for convenience.

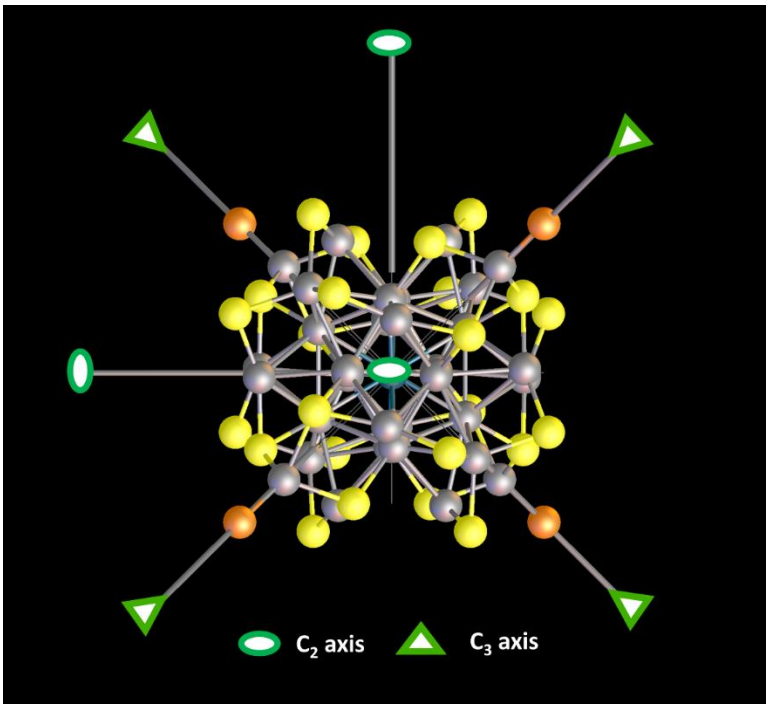

Figure S5 Rotational axis in the kernel of Ag_{33} nanoparticle. The framework consists of 4 C_3 and 3 C_2 rotational axis with no additional inversion or reflection operations, indicating the symmetries of the particle falling in ***T*** point group.

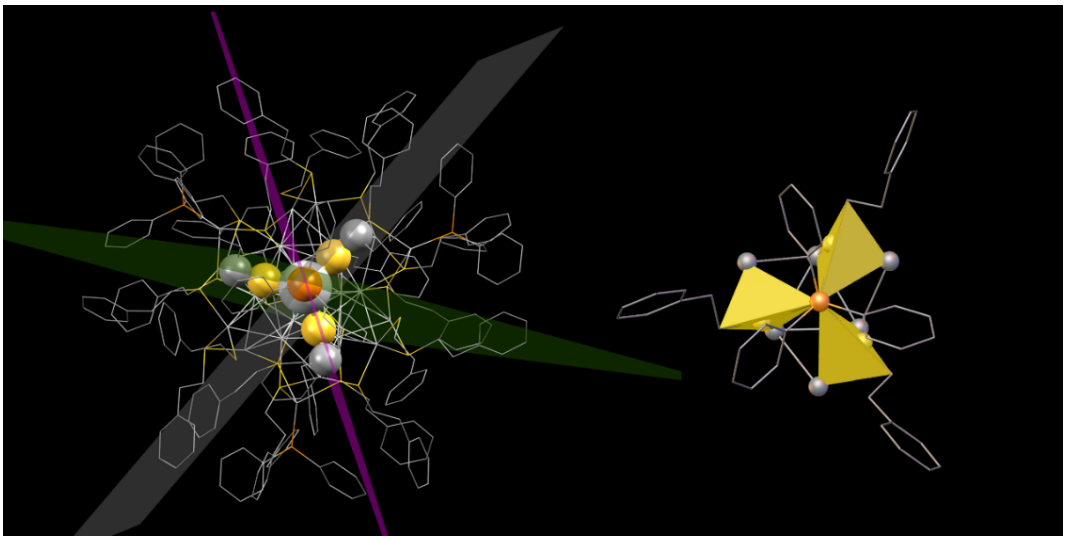

Figure S6 Geometries of bonding features for four coordinated S atoms: co-plane (left) and polyhedron (right) illustrations

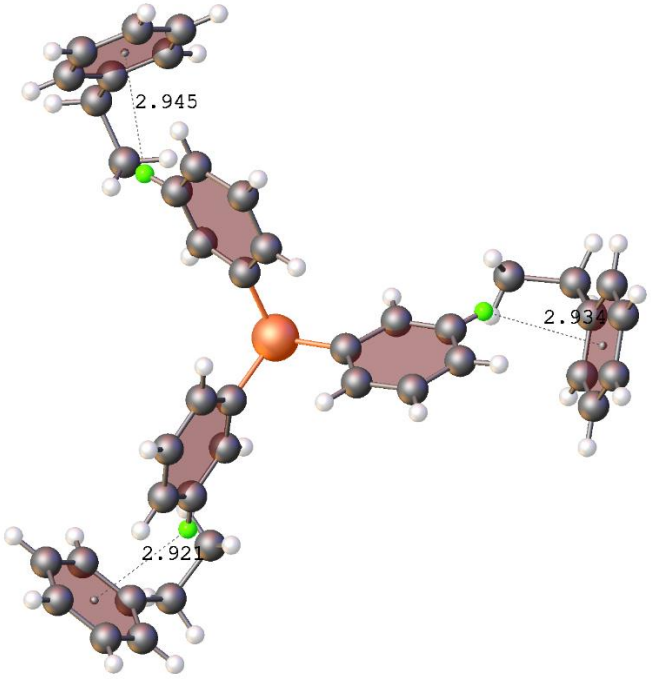

Figure S7 C-H···π interactions between phenyl groups in PPh_3 sulfur ligands. The un-involved Ag, Pd and S atoms were omitted for simplification. One of the meta-H (the green one) in the phenyls of PPh_3 is found interacting between the neighboring phenyl ring of phenyl ethyl S (S_2) ligand, with bonding length of 2.93 ±0.2 Å.

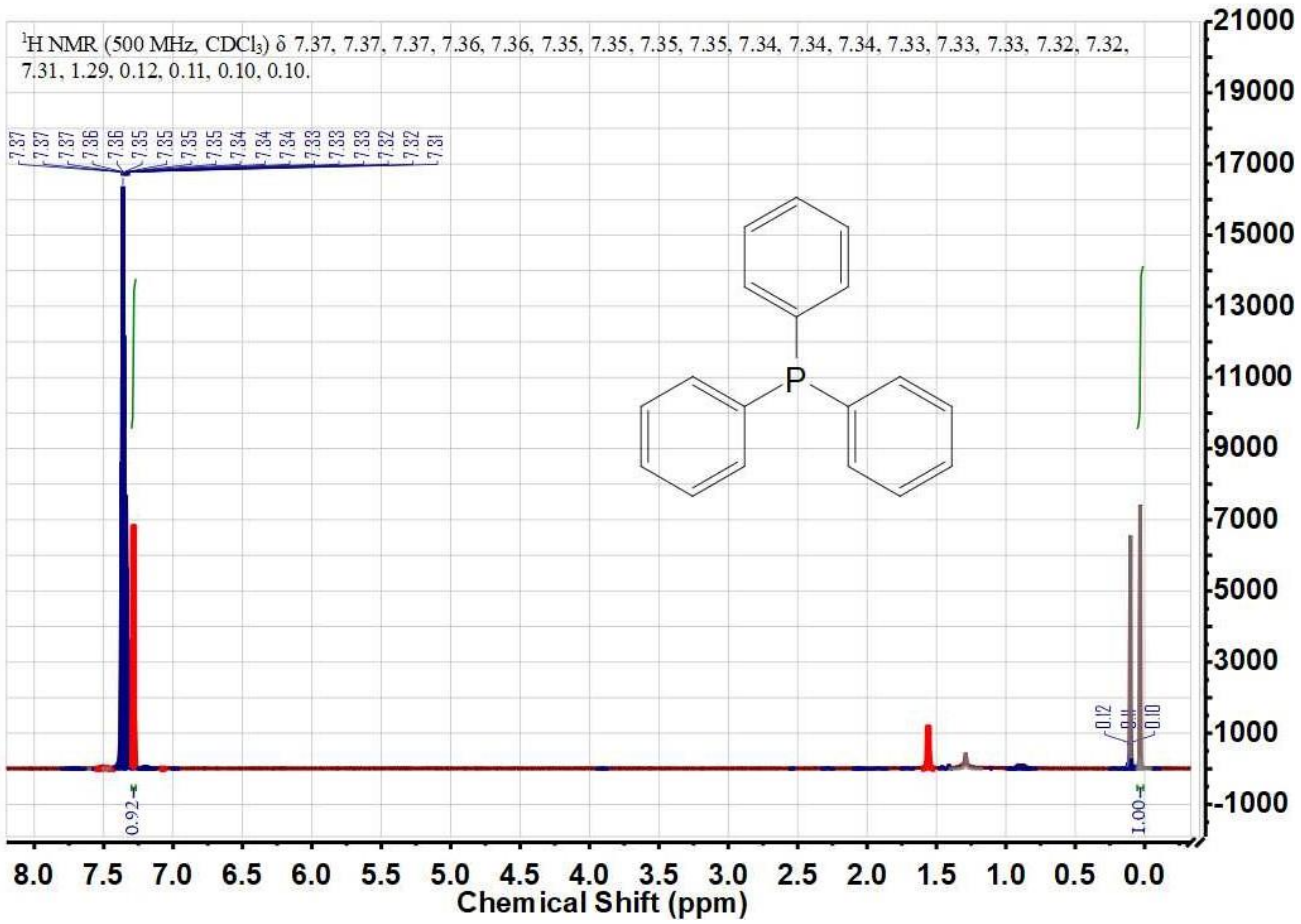

Figure S8 ^{1}H NMR spectrum of PPh_3 acquired in $CDCl_3$.

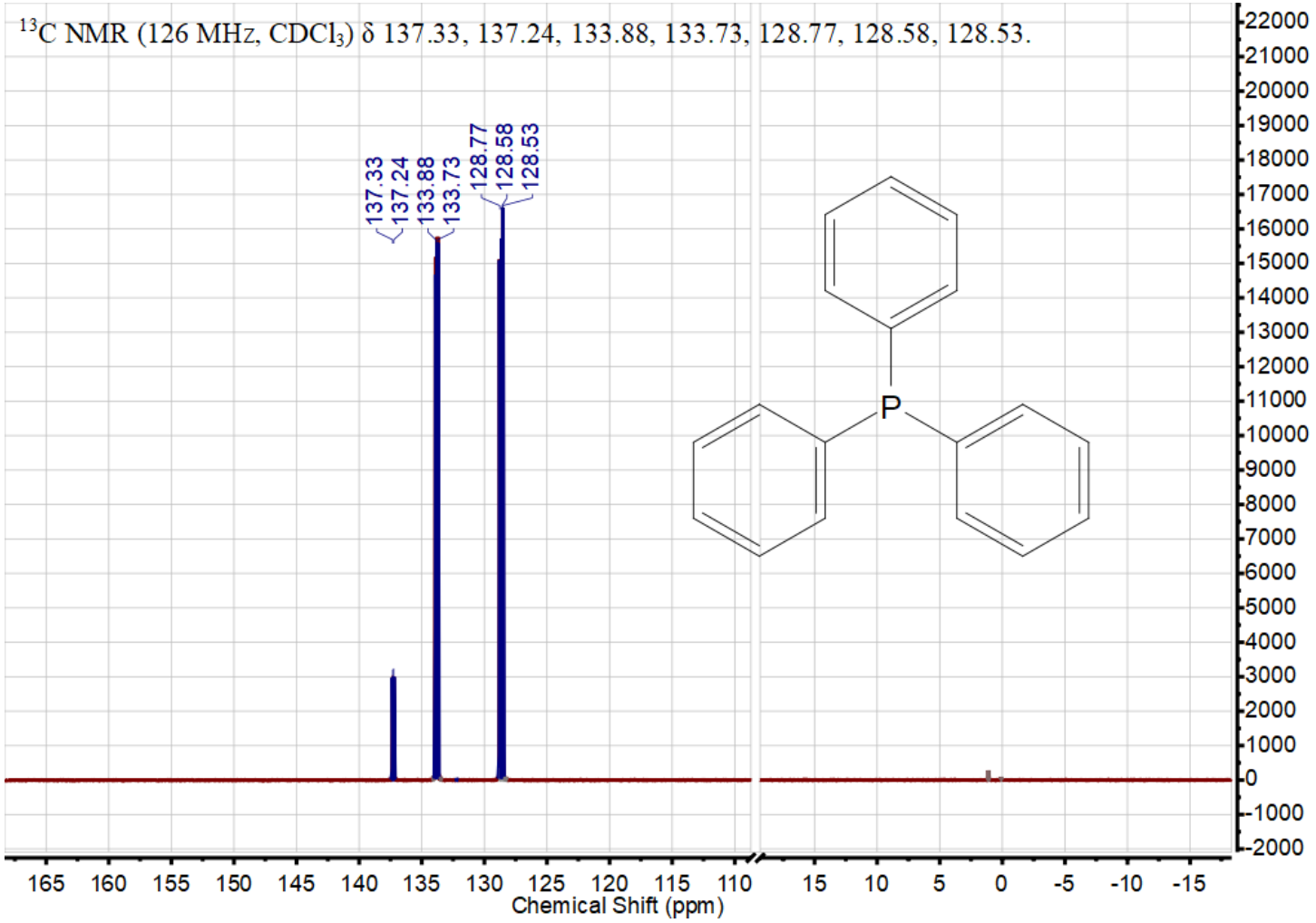

Figure S9 ^{13}C NMR spectrum of PPh_3 acquired in $CDCl_3$.

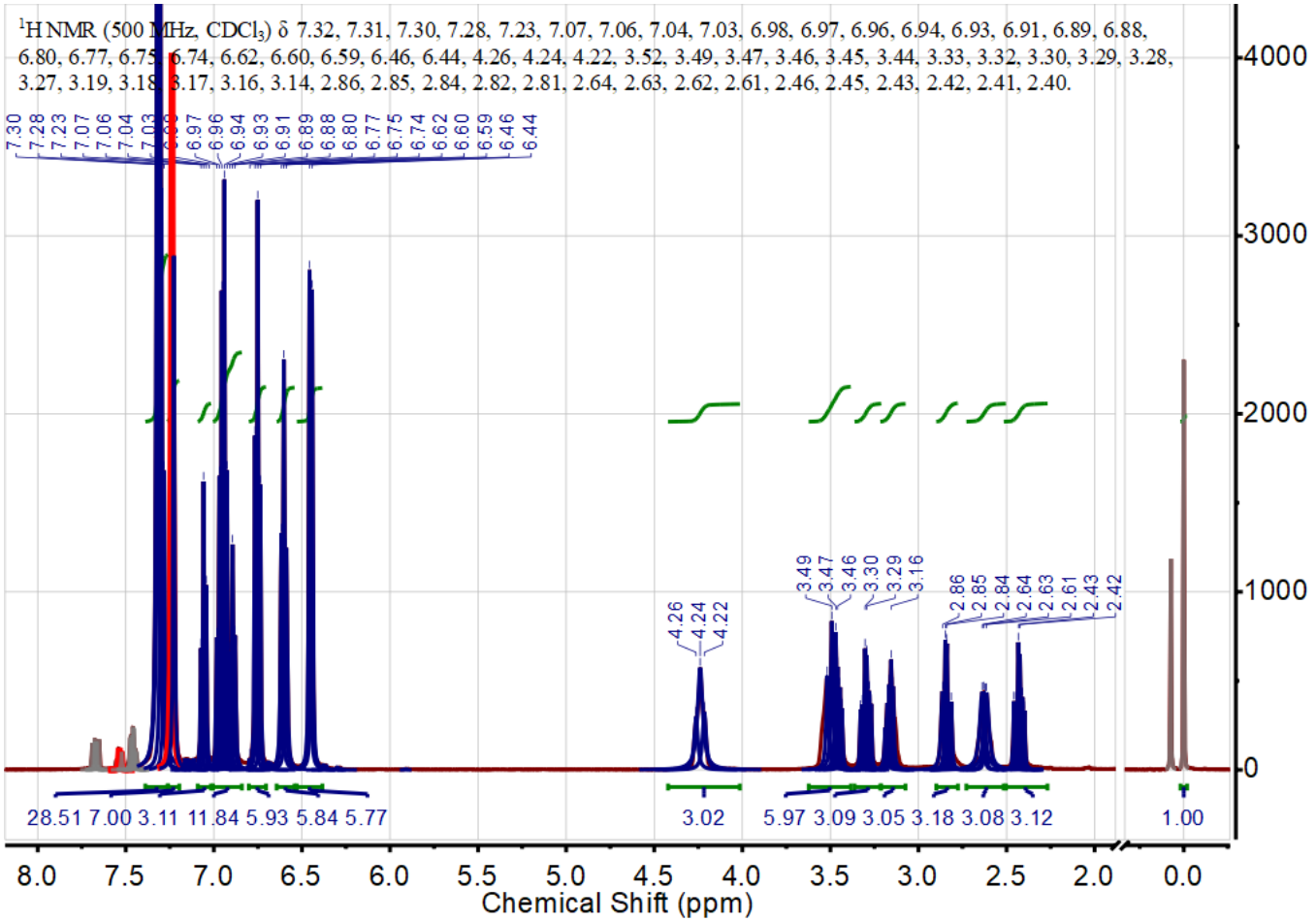

Figure S10 ^{1}H NMR of the as-obtained crystals acquired in $CDCl_3$ with additional PPh_3 added to stabilize the clusters. The concentration of PPh_3 is 10 mg/mL.

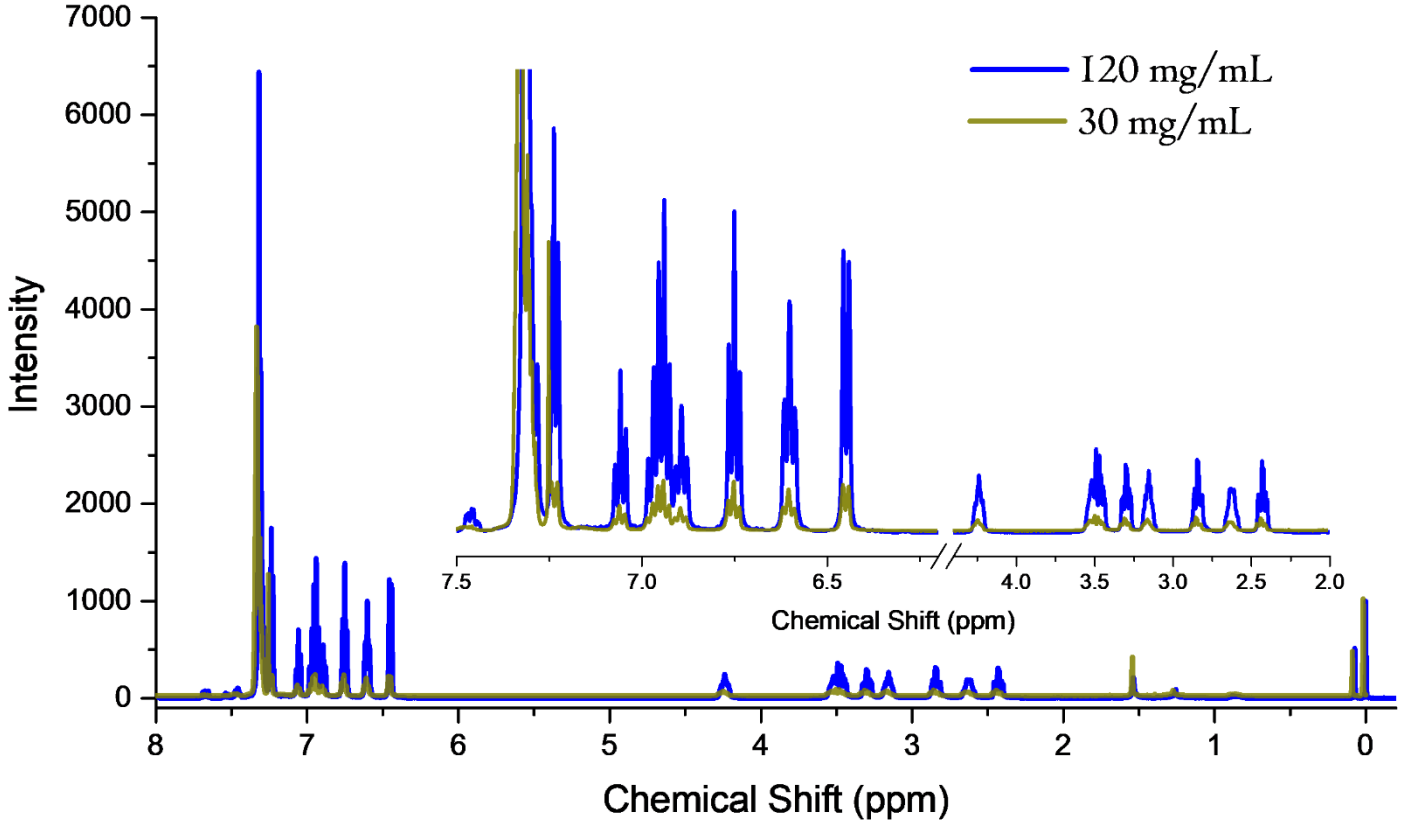

Figure S11 ^{1}H NMR of the as-obtained crystals acquired in $CDCl_3$ with different concentration of the clusters.

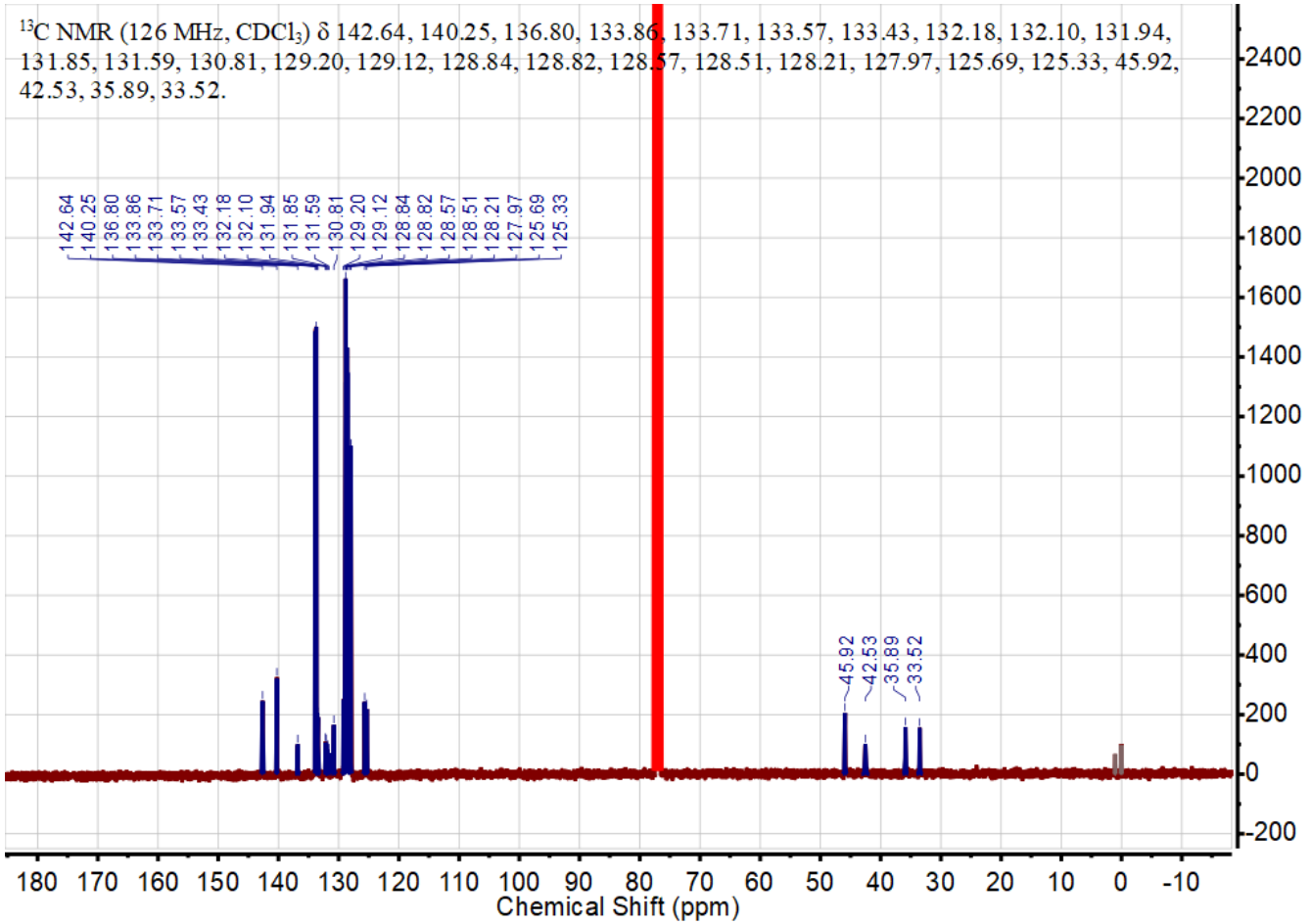

Figure S12 ^{13}C NMR of the as-obtained crystals acquired in $CDCl_3$ with additional PPh_3 added to stabilize the clusters. The concentration of PPh_3 is 10 mg/mL.

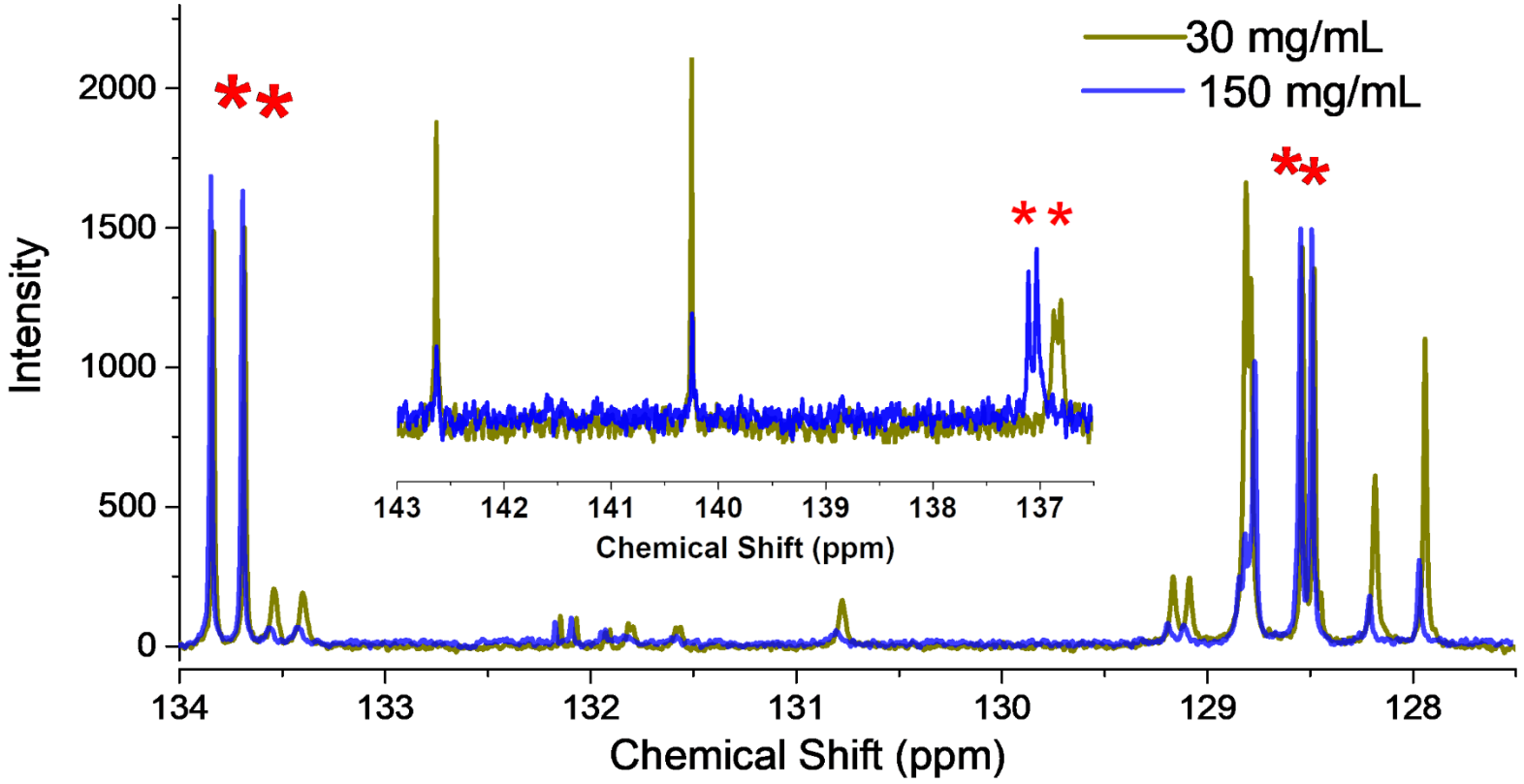

Figure S13 ^{13}C NMR of the as-obtained crystals acquired in $CDCl_3$ with different concentration of the clusters. The resonance signal attributes to the dissociate PPh_3.

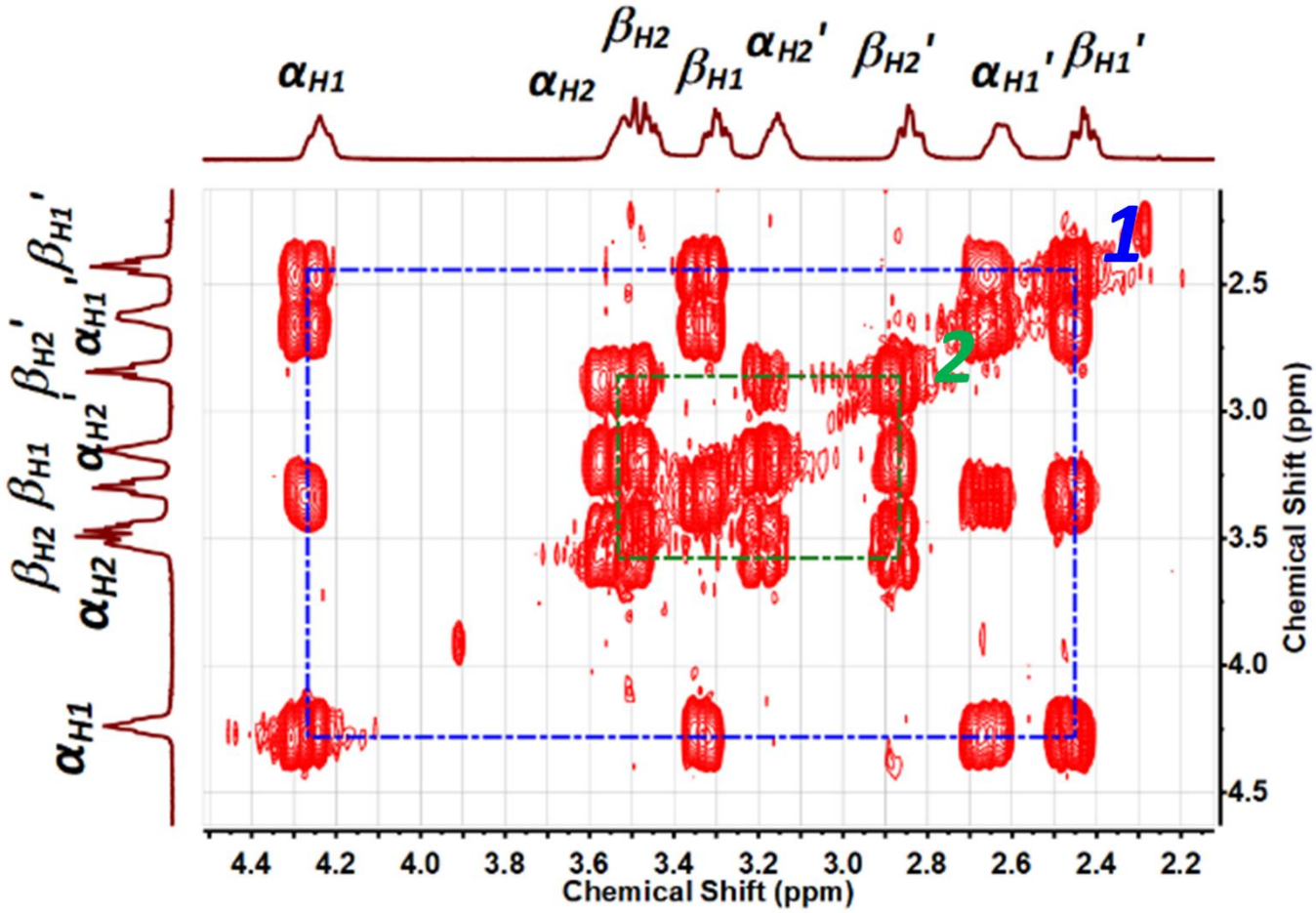

Figure S14 ^{1}H-^{1}H COSY spectra of the methylene groups in thiol ligands of Ag_{33} nanocluster.

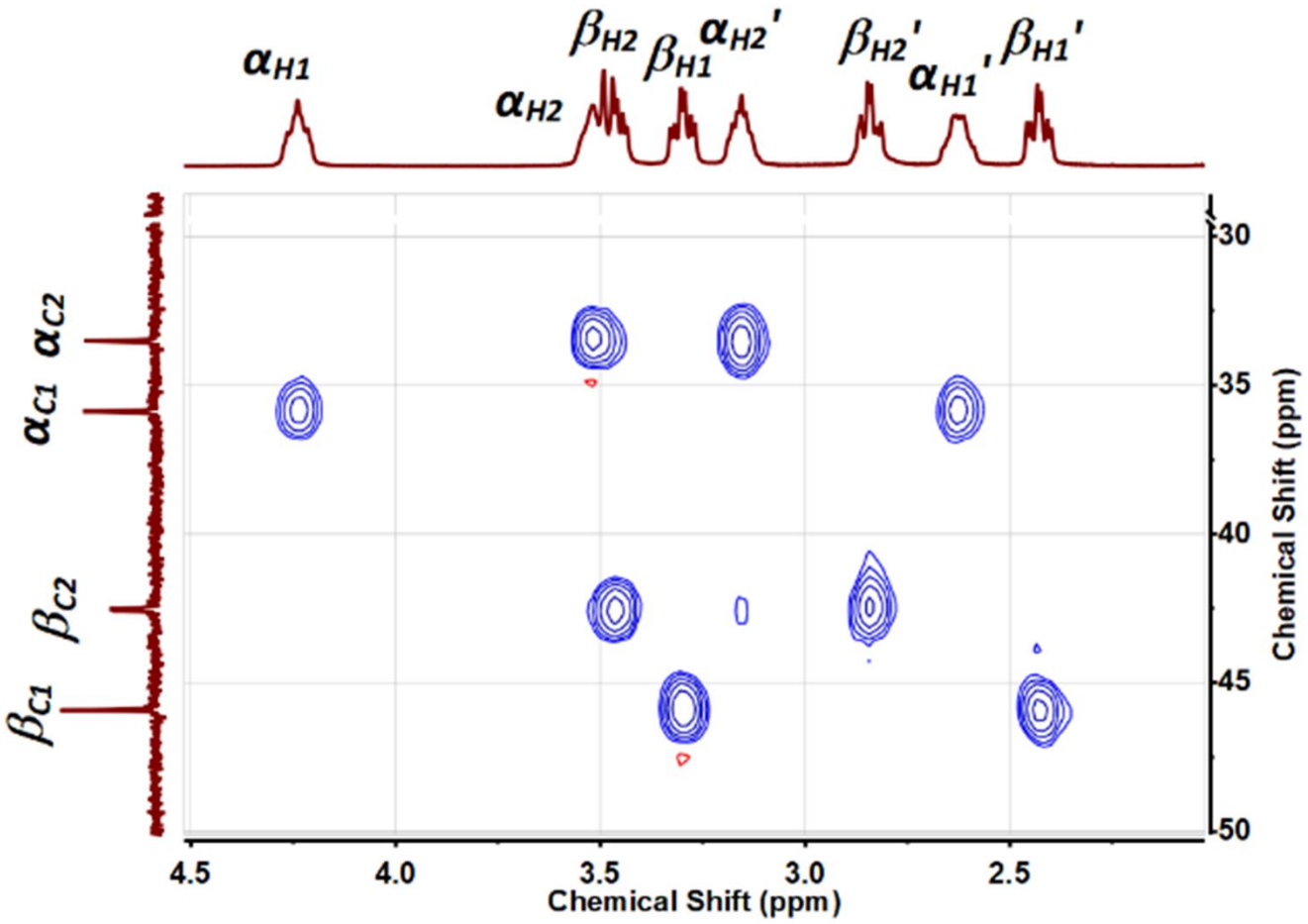

Figure S15 ^{1}H-^{13}C HSQC spectra of the methylene groups in thiol ligands of Ag_{33} nanocluster.

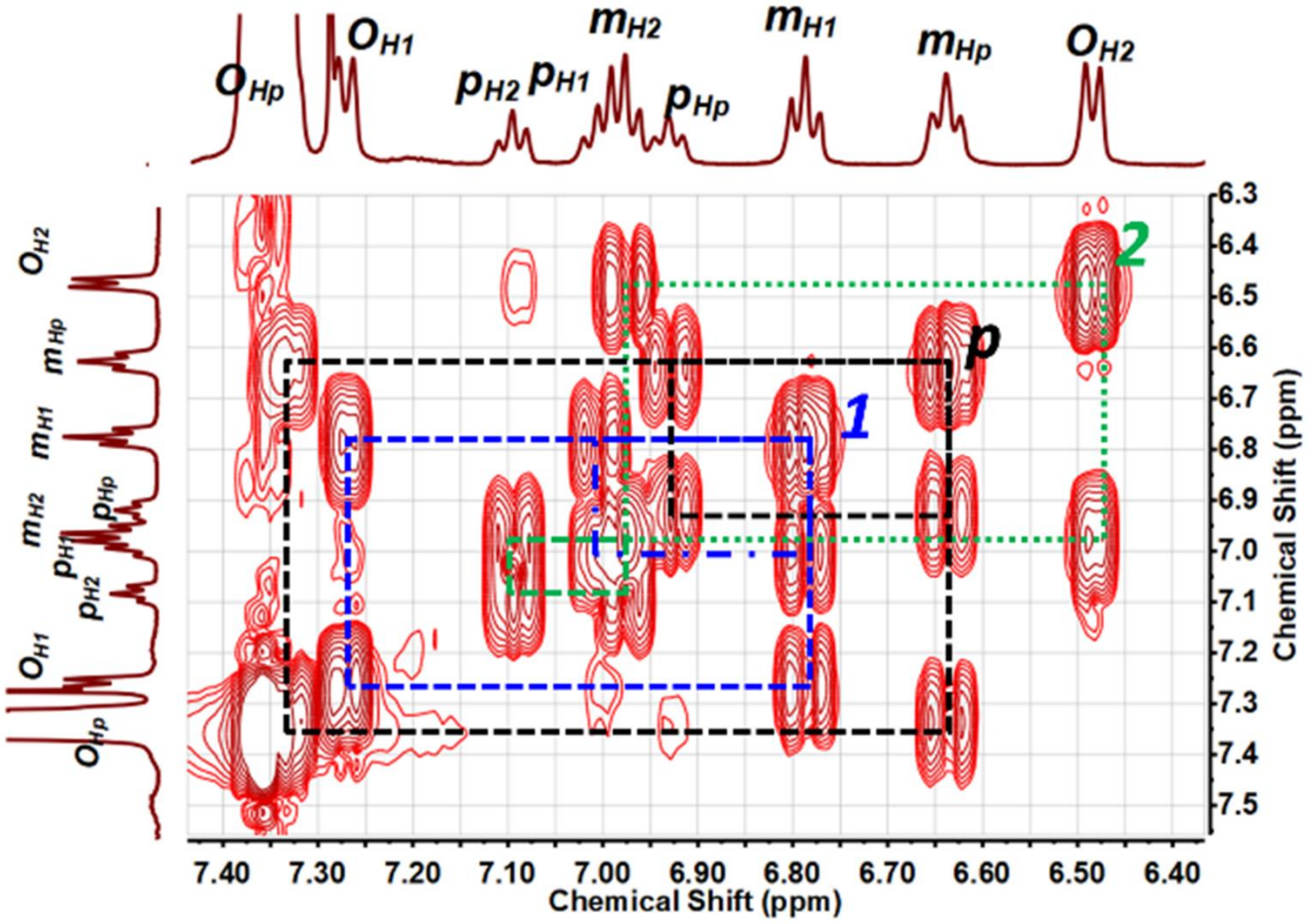

Figure S16 ^{1}H-^{1}H COSY spectra of the phenyl groups in the ligands of Ag_{33} nanocluster.

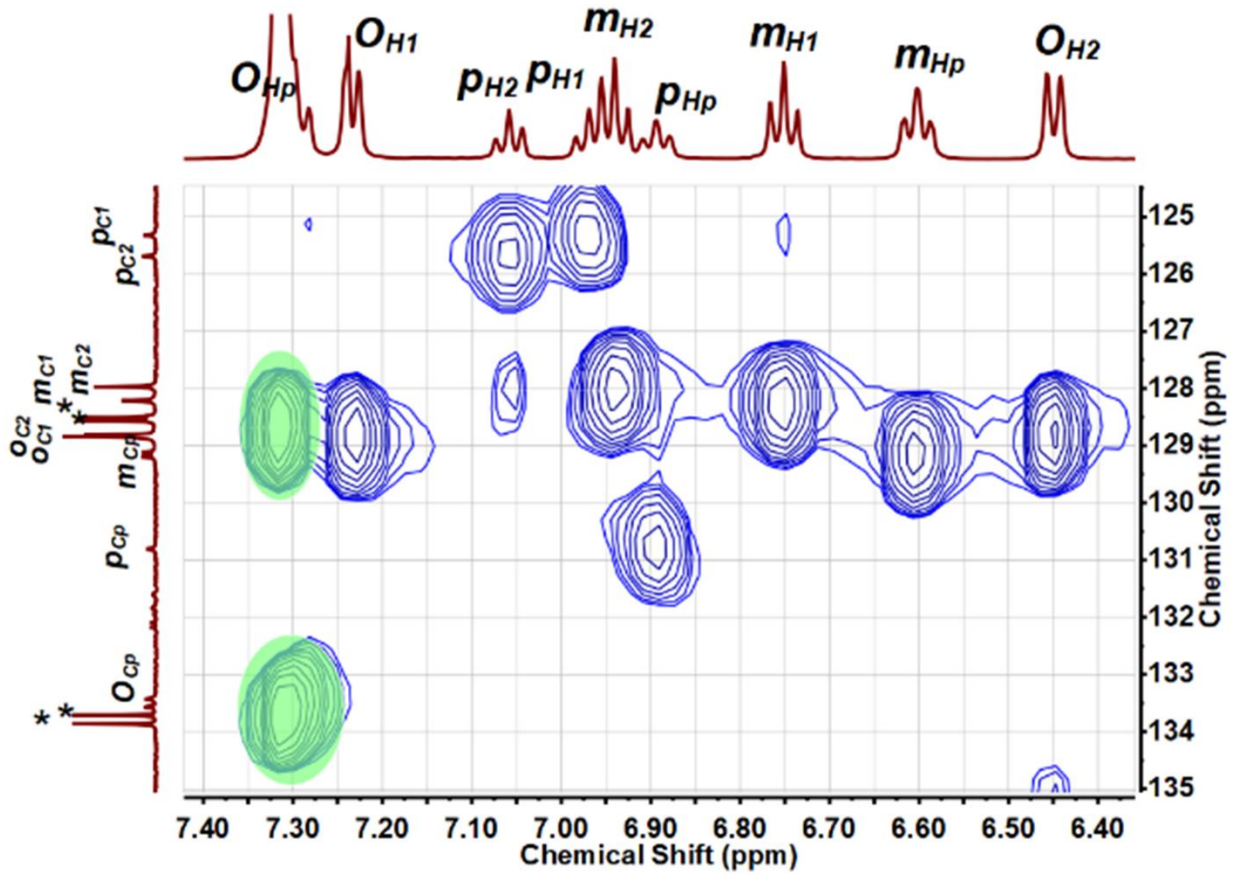

Figure S17 ^{1}H-^{13}C HSQC spectra of phenyl groups in the ligands of Ag_{33} nanocluster. The black '*' denote atoms in dissociative PPh_3 in solution.

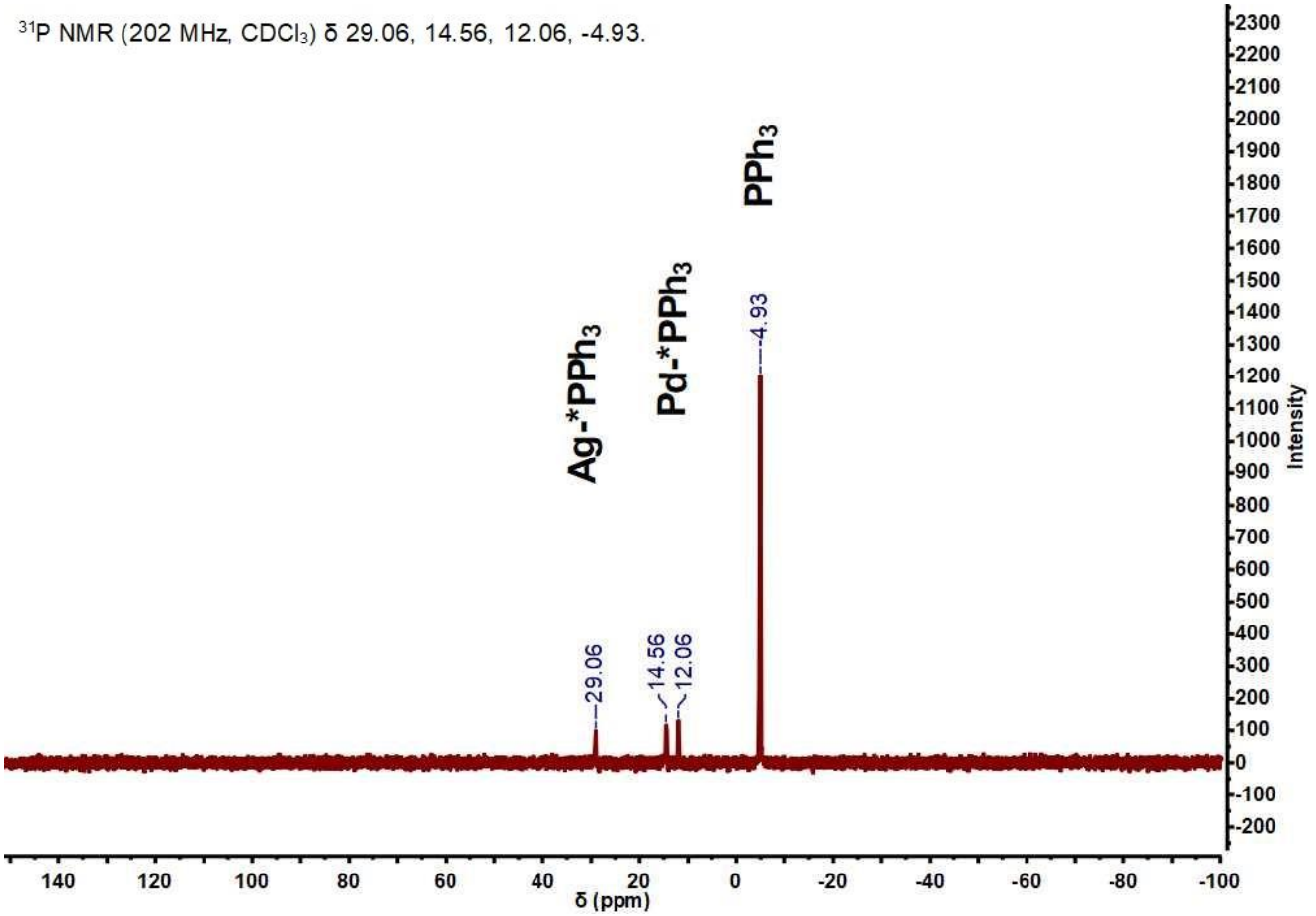

Figure S18 ^{31}P NMR of the as-obtained crystals acquired in $CDCl_3$ with additional PPh_3 added to stabilize the clusters. The concentration of PPh_3 is 10 mg/mL.

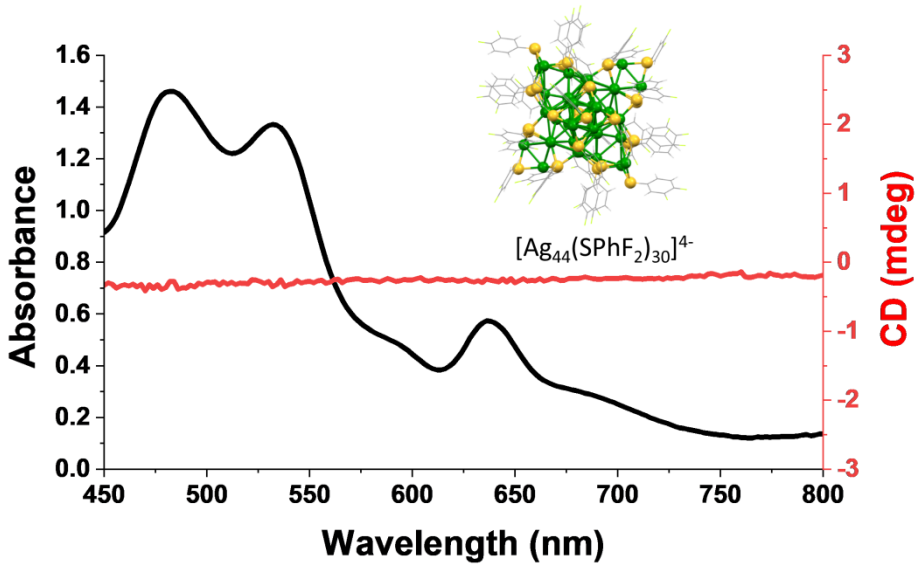

Figure S19. UV-visible absorption and circular dichroism spectrum of $[Ag_{44}(SPhF_2)_{30}]^{4-}$ nanocluster. The Ag_{44} nanocluster is synthesized by referring the previous report[8].

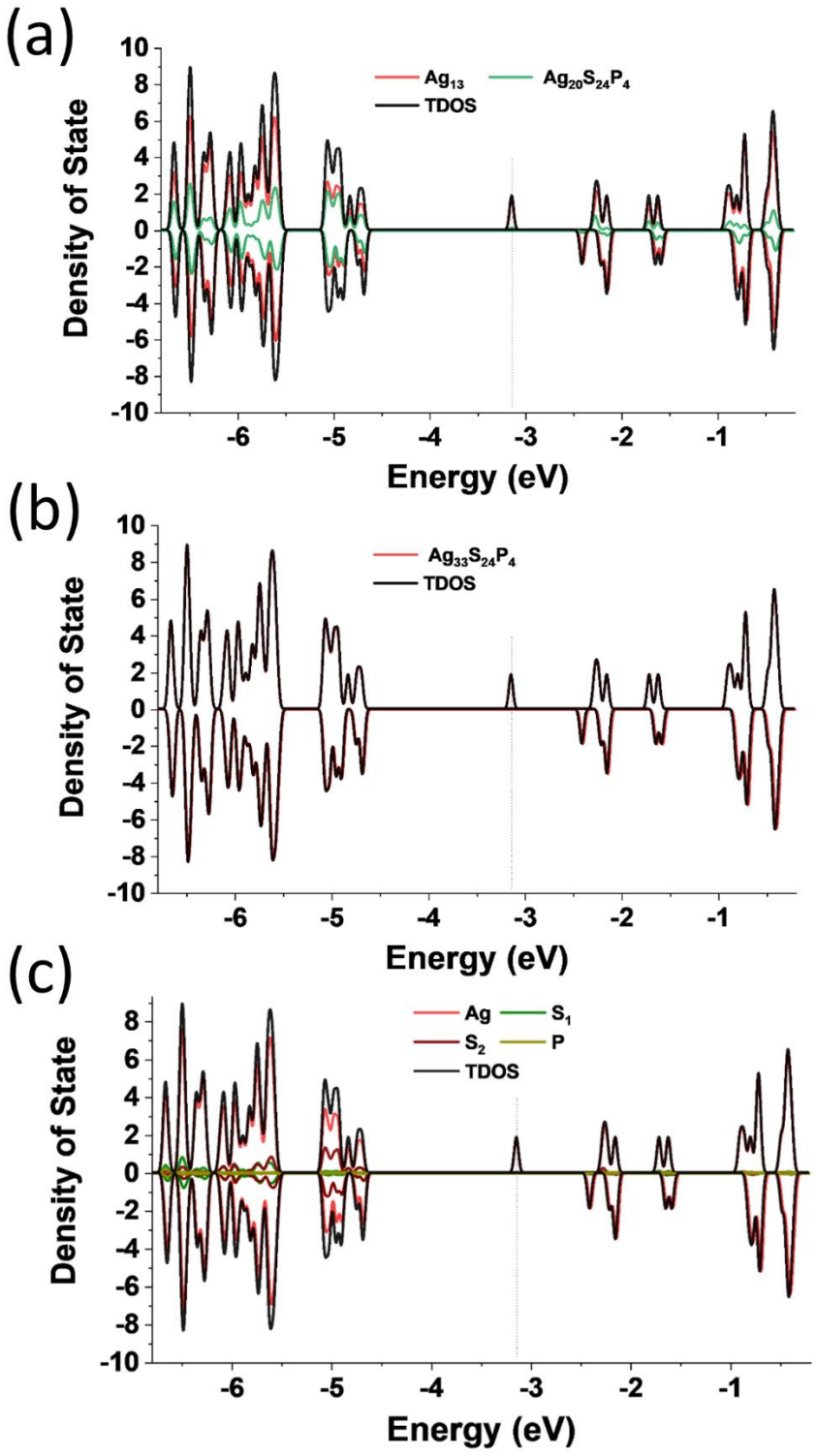

Figure S20 Projected density of states (PDOS) plot of Ag_{33} nanocluster: PDOS for Ag_{13} icosahedron core and $Ag_{20}S_{24}P_4$ shell vs. total partial density of states (TDOS) of $Ag_{33}(SCH_3)_{24}(PCH_3)_4$(a); PDOS for kernel atoms (Ag, S, P) vs. TDOS of $Ag_{33}(SCH_3)_{24}(PCH_3)_4$(b); PDOS for Ag, S and P atoms vs. TDOS of $Ag_{33}(SCH_3)_{24}(PCH_3)_4$ (c).

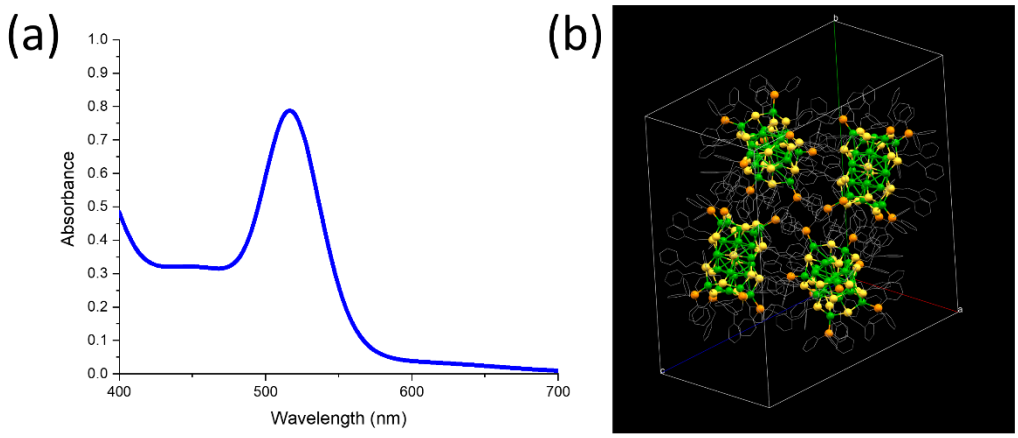

Figure S21 Optical absorption spectrum of the products synthesized *via* the reduction of a mixture of Ag, phenylethanethiol and triphenylphosphine by $NaBH_4$ aqueous solution in the absence of Pd regent (a) and the crystal structure of the as obtained products (b). The as-synthesized products is previously reported Ag_{23} nanocluster[9].

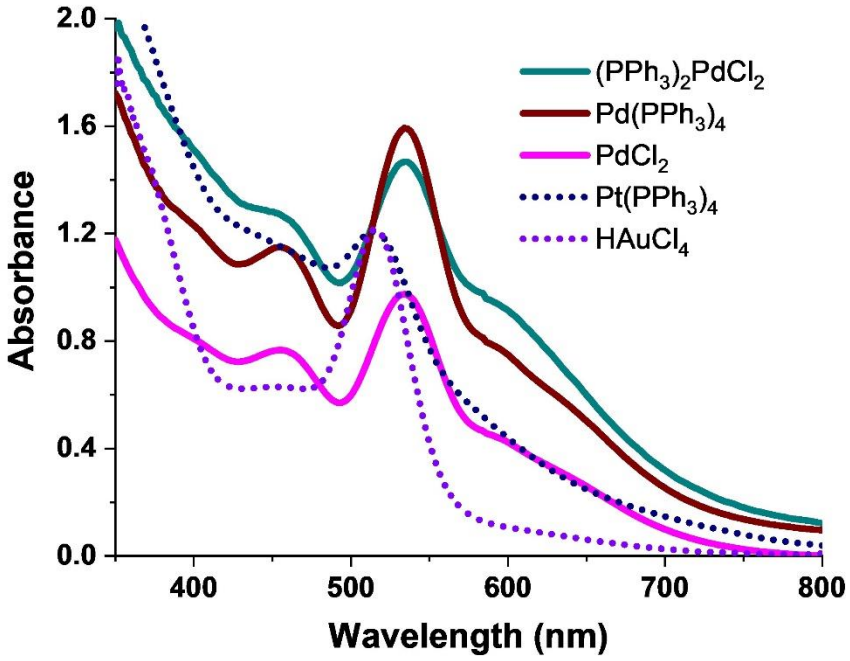

Figure S22 UV-visible adsorption spectra of products obtained in the presence of $(PPh_3)_2PdCl_2$, $Pd(PPh_3)_4$, $PdCl_2$,$Pt(PPh_3)_4$ and $HAuCl_4$, respectively.

Table S1. Crystal data and structure refinement for $Ag_{33}(SCH_2CH_2Ph)_{24}(PPh)_4$

Identification code	$Ag_{33}(SCH_2CH_2Ph)_{24}(PPh)_4$
Empirical formula	$C_{1083.23}H_{1053.8}Ag_{107.25}Cl_{16.19}P_{28.41}Pd_4S_{78}$
Formula weight	30021.50
Temperature/K	100.00(10)
Crystal system	cubic
Space group	P-43n
a/Å	39.92740(10)
b/Å	39.92740(10)
c/Å	39.92740(10)
α/°	90
β/°	90
γ/°	90
Volume/Å^3	63652.2(5)
Z	2
ρ_{calc}g/cm^3	1.566
μ/mm^{-1}	15.505
F(000)	29454.0
Crystal size/mm^3	0.5 × 0.2 × 0.1
Radiation	CuKα (λ = 1.54178)
2Θ range for data collection/°	4.948 to 147.696
Index ranges	$-24 \le h \le 49$, $-37 \le k \le 25$, $-23 \le l \le 44$
Reflections collected	74430
Independent reflections	18759 [R_{int} = 0.0498, R_{sigma} = 0.0512]
Data/restraints/parameters	18759/350/958
Goodness-of-fit on F^2	1.052
Final R indexes [I>=2σ (I)]	R_1 = 0.0567, wR_2 = 0.1594
Final R indexes [all data]	R_1 = 0.0781, wR_2 = 0.1771
Largest diff. peak/hole / e Å^{-3}	1.80/-0.70
Flack parameter	0.028(6)

Table S2. Ag, Pd contends in the crystals according to ICP-MS and SCXRD analysis

	Ag	**Pd**	**Ag/Pd (mole ratio)**
ICP-MS (mg/L)	21.29	0.50	41.16
SCXRD (mole No.)	41.25	1	41.25

Table S3. Comparisons of bond lengths in Ag_{13} icosahedron with the similar structures in the reported nanocluster structures.

Cluster structure	Icosahedron structure[a]	Bond length (Å)		Refs
		$M_{cen.}$-M_{ico}[b]	$M_{ico.}$-M_{ico}	
$Ag_{33}(SR)_{24}(PPh)_4$	Ag_{12}**[**Ag**]**	2.78-2.80	2.82-3.08	This work
$Ag_{24}Pd(SR)_{18}$	Ag_{12}**[**Pd**]**	2.73-2.77	2.82-2.97	10-11
$Ag_{24}Pt(SR)_{18}$	Ag_{12}**[**Pt**]**	2.73-2.78	2.83-3.00	10-11
$Ag_{25}(SR)_{18}$	Ag_{12}**[**Ag**]**	2.74-2.79	2.82-3.00	12
$Ag_{24}Au(SR)_{18}$	Ag_{12}**[**Au**]**	2.74-2.80	2.86-2.98	11, 13
$Ag_{29}(BDT)_{12}(TPP)_4$	Ag_{12}**[**Ag**]**	2.75-2.77	2.83-2.97	14
$Ag_{44}(SR)_{20}$	Ag_{12}[c]	_ _	2.80-2.87	8, 15
$Au_{12}Ag_{32}(SR)_{20}$	Au_{12}[c]	_ _	2.75-2.82	8
$Au_{25}(SR)_{18}$	Au_{12}**[**Au**]**	2.76-2.79	2.80-2.99	16-17
$Au_{24}Cd(SR)_{18}$	$(Au_{11/12}Cd_{1/12})_{12}$**[**Au**]**	2.77-2.80	2.80-3.03	18

[a]. The icosahedron structure is formatted by the atoms compositions. Centered atom in the icosahedron is bracketed by **[ ]** for distinguishing.

[b]. A_{cen} and A_{ico} denote the centered atom in the icosahedron and atom on the vertex of the icosahedron, respectively.

[c]. No centered atom in the structure.

Table S4. Comparisons of bond lengths for Ag-S in Ag_{33} nanoparticles measured from Single Crystal X-Ray Diffraction (SCXRD) and DFT calculations.

Bond type[a]	Bond length (Å)	
	From SCXRD	From DFT
S_1-Ag_T	2.56-2.58	2.676
S_1-Ag_I	2.50-2.53	2.600
S_1-Ag_s	2.42-2.43	2.452
S_2-Ag_s	~2.54	2.417
S_2-Ag_B	2.36~2.37	2.652

[a]. S_1 and S_2 denote the asterisked sulfur atoms in $-S^*$-Ag-P and -S^*-Ag-S-, respectively. The sliver atoms are denoted as: Ag_T, Ag atom in -Ag-P motif; Ag_I, Ag atoms in $Ag_{12}Pd$ icosahedron; Ag_O,Ag atom outside the plane determined by P, S_1 and α-C connecting to S_1 atoms (see Figure 2b and c in the main article).

Table S5 The assignment and integrals of methylene and phenyl groups in the ^{1}H NMR spectrum with TMS as CS and quant. reference.

Peak	Chemical shift (ppm)	Assignment[a]	Integral[b]
0	0	H in TMS	1
1	2.43	$\boldsymbol{\beta_{H1}'}$	3
2	2.64	$\boldsymbol{\alpha_{H1}'}$	3
3	2.84	$\boldsymbol{\beta_{H2}'}$	3
4	3.16	$\boldsymbol{\alpha_{H2}'}$	3
5	3.30	$\boldsymbol{\beta_{H1}}$	3
6	3.48	$\boldsymbol{\beta_{H2}}$ $\boldsymbol{\alpha_{H2}}$	6
7	4.24	$\boldsymbol{\alpha_{H1}}$	3
8	6.45	$\boldsymbol{o_{H2}}$	6
9	6.60	$\boldsymbol{m_{Hp}}$	6
10	6.75	$\boldsymbol{m_{H1}}$	6
11	6.95	$\boldsymbol{p_{Hp}}$ $\boldsymbol{m_{H2}}$ $\boldsymbol{p_{H1}}$	12
12	7.06	$\boldsymbol{p_{H2}}$	3
13	7.24	$\boldsymbol{o_{H1}}$	6[c]
14	7.32	$\boldsymbol{o_{Hp}}$ H in $Pd(PPh_3)_4$] H in PPh_3	29

[a]. we use the carbon site labels to locate the protons in the ligands. The carbon atoms in methylene groups relative to the sulfur atom are labeled as $\boldsymbol{\alpha}$ and $\boldsymbol{\beta}$. The carbon atoms in phenyl groups are labeled as ***o***, ***m*** and ***p*** for the sites in ortho-position, meta-position and para-positon, respectively. The subscripts following are used to distinguish the atoms associated with which type ligands, where 1, 2 correspond to the ligands of $PhCH_2CH_2S$- with S atoms coordinated with three Ag atoms, two Ag atoms and ***p*** denotes the ligand of PPh_3. The two protons in methylene group are arbitrarily distinguished by a quotation mark. See details in Figure 3.

[b].The integrals are rounded off according to the integration in Figure S8.

[c]. The integral '6' comes from '7.0 (the corresponding integral in Figure S8)-0.92 (the contributions from $CDCl_3$, see Figure S7) = 6.08'.

Table S6 The assignment carbon atoms in the ^{13}C NMR spectrum.

Peak	Chemical shift (ppm)	Assignment[a]
1	33.52	α_{C2}
2	35.89	α_{C1}
3	42.53	β_{C2}
4	45.92	β_{C1}
5	125.33	p_{C1}
6	125.69	p_{C2}
7	127.97	m_{C2}
8	128.21	m_{C1}
9	128.51	PPh_3
10	128.57	
13	128.82	o_{C2}
14	128.84	o_{C1}
15	129.12	m_{Cp}
16	129.20	
17	130.81	p_{Cp}
18	136.80	PPh_3
19	136.87	
20	140.24	C*-C[b]
21	142.64	C*-P*[c]

[a]. The labels of assignments are in accord with Table S5. For more details, see Table S5 and Figure 3.

[b]. denotes the carbon atoms in phenyl groups which connect to methylene in $PhCH_2CH_2S$-ligands.

[c]. denotes the carbon atoms which directly connected by phosphorus atoms in the coordinated PPh_3 ligands.

Reference

1. Muniz-Miranda, F.; Menziani, M. C.; Pedone, A., DFT and TD-DFT assessment of the structural and optoelectronic properties of an organic-Ag_{14} nanocluster. *J. Phys. Chem. A* **2015,** *119* (21), 5088-98.

2. M. J. Frisch, G. W. T., H. B. Schlegel, G. E. Scuseria, ; M. A. Robb, J. R. C., G. Scalmani, V. Barone, ; G. A. Petersson, H. N., X. Li, M. Caricato, A. V. Marenich, ; J. Bloino, B. G. J., R. Gomperts, B. Mennucci, H. P. Hratchian, ; J. V. Ortiz, A. F. I., J. L. Sonnenberg, D. Williams-Young, ; F. Ding, F. L., F. Egidi, J. Goings, B. Peng, A. Petrone, ; T. Henderson, D. R., V. G. Zakrzewski, J. Gao, N. Rega, ; G. Zheng, W. L., M. Hada, M. Ehara, K. Toyota, R. Fukuda, ; J. Hasegawa, M. I., T. Nakajima, Y. Honda, O. Kitao, H. Nakai, ; T. Vreven, K. T., J. A. Montgomery, Jr., J. E. Peralta, ; F. Ogliaro, M. J. B., J. J. Heyd, E. N. Brothers, K. N. Kudin, ; V. N. Staroverov, T. A. K., R. Kobayashi, J. Normand, ; K. Raghavachari, A. P. R., J. C. Burant, S. S. Iyengar, ; J. Tomasi, M. C., J. M. Millam, M. Klene, C. Adamo, R. Cammi, ; J. W. Ochterski, R. L. M., K. Morokuma, O. Farkas, ; J. B. Foresman, a. D. J. F., Gaussian 16 Revision B.01 (2016) *Gaussian Inc.: Wallingford CT.*

3. Lu, T.; Chen, F., Multiwfn: a multifunctional wavefunction analyzer. *J. Comput. Chem.* **2012,** *33* (5), 580-92.

4. Rigaku Oxford Diffraction, x., CrysAlisPro Software system, version 1.171.39.46,. *Rigaku Corporation, Oxford, UK.*

5. Dolomanov, O. V.; Bourhis, L. J.; Gildea, R. J.; Howard, J. A. K.; Puschmann, H., OLEX2: a complete structure solution, refinement and analysis program. *J. Appl. Crystallogr.* **2009,** *42* (2), 339-341.

6. Sheldrick, G. M., A short history of SHELX. *Acta Crystallogr A* **2008,** *64* (Pt 1), 112-22.

7. Sheldrick, G. M., Crystal structure refinement with SHELXL. *Acta Crystallogr C Struct Chem* **2015,** *71* (Pt 1), 3-8.

8. Yang, H.; Wang, Y.; Huang, H.; Gell, L.; Lehtovaara, L.; Malola, S.; Hakkinen, H.; Zheng, N., All-thiol-stabilized Ag_{44} and $Au_{12}Ag_{32}$ nanoparticles with single-crystal structures. *Nat. Commun.* **2013,** *4* (1), 2422.

9. Liu, C.; Li, T.; Abroshan, H.; Li, Z.; Zhang, C.; Kim, H. J.; Li, G.; Jin, R., Chiral Ag_{23} nanocluster with open shell electronic structure and helical face-centered cubic framework. *Nat. Commun.* **2018,** *9* (1), 744.

10. Yan, J.; Su, H.; Yang, H.; Malola, S.; Lin, S.; Hakkinen, H.; Zheng, N., Total Structure and Electronic Structure Analysis of Doped Thiolated Silver $[MAg_{24}(SR)_{18}]^{2-}$ (M = Pd, Pt) Clusters. *J. Am. Chem. Soc.* **2015,** *137* (37), 11880-3.

11. Liu, X.; Yuan, J.; Yao, C.; Chen, J.; Li, L.; Bao, X.; Yang, J.; Wu, Z., Crystal and Solution Photoluminescence of $MAg_{24}(SR)_{18}$ (M = Ag/Pd/Pt/Au) Nanoclusters and Some Implications for the Photoluminescence Mechanisms. *J. Phys. Chem. C* **2017,** *121* (25), 13848-13853.

12. Joshi, C. P.; Bootharaju, M. S.; Alhilaly, M. J.; Bakr, O. M., $[Ag_{25}(SR)_{18}]^-$: The "Golden" Silver Nanoparticle. *J. Am. Chem. Soc.* **2015,** *137* (36), 11578-81.

13. Bootharaju, M. S.; Joshi, C. P.; Parida, M. R.; Mohammed, O. F.; Bakr, O. M., Templated Atom-Precise Galvanic Synthesis and Structure Elucidation of a $[Ag_{24}Au(SR)_{18}]^-$ Nanocluster. *Angew. Chem.* **2016,** *128* (3), 934-938.
14. AbdulHalim, L. G.; Bootharaju, M. S.; Tang, Q.; Del Gobbo, S.; AbdulHalim, R. G.; Eddaoudi, M.; Jiang, D. E.; Bakr, O. M., $Ag_{29}(BDT)_{12}(TPP)_4$: A Tetravalent Nanocluster. *J. Am. Chem. Soc.* **2015,** *137* (37), 11970-5.
15. Desireddy, A.; Conn, B. E.; Guo, J.; Yoon, B.; Barnett, R. N.; Monahan, B. M.; Kirschbaum, K.; Griffith, W. P.; Whetten, R. L.; Landman, U.; Bigioni, T. P., Ultrastable silver nanoparticles. *Nature* **2013,** *501* (7467), 399-402.
16. Heaven, M. W.; Dass, A.; White, P. S.; Holt, K. M.; Murray, R. W., Crystal structure of the gold nanoparticle $[N(C_8H_{17})_4][Au_{25}(SCH_2CH_2Ph)_{18}]$. *J. Am. Chem. Soc.* **2008,** *130* (12), 3754-5.
17. Zhu, M.; Aikens, C. M.; Hollander, F. J.; Schatz, G. C.; Jin, R., Correlating the crystal structure of a thiol-protected Au_{25} cluster and optical properties. *J. Am. Chem. Soc.* **2008,** *130* (18), 5883-5.
18. Yao, C.; Lin, Y. J.; Yuan, J.; Liao, L.; Zhu, M.; Weng, L. H.; Yang, J.; Wu, Z., Mono-cadmium vs Mono-mercury Doping of Au_{25} Nanoclusters. *J. Am. Chem. Soc.* **2015,** *137* (49), 15350-3.